



Combined effects of deep eutectic solvent and microwave energy treatments on cellulose fiber extraction from hemp bast

Bulbul Ahmed · Jaegyoung Gwon · Manish Thapaliya · Achyut Adhikari ·
Suxia Ren · Qinglin Wu

Received: 20 October 2022 / Accepted: 28 January 2023
© The Author(s), under exclusive licence to Springer Nature B.V. 2023

Abstract Extracting pure cellulose fibers from hemp fibers for value-added applications like industrial textile requires the removal of non-cellulosic gummy substances. However, traditional degumming methods are largely limited due to their long process time, high energy consumption, and detrimental environmental pollution. Herein, several deep eutectic solvents (DESs) combined with microwave energy (MWE) were explored to degum hemp fibers without any further treatment. The purified hemp cellulose fibers were systematically characterized using advanced analytical techniques. Results revealed that the synergetic effect of combined

MWE-DES treatment was capable of removing non-cellulosic components such as lignin, hemicellulose, amorphous cellulose, and impurities from the fiber structure without damaging the cellulose structure. MWE-DES treated fibers had higher thermal stability (maximum degradation temperature of MWE-DES treated fibers reached 356 °C), lower residual lignin content (2.88%), and higher crystallinity (83.27% for choline chloride and urea DES). Moreover, MWE-DES treated fibers showed the inhibition of bacterial growth, comparable with that from untreated raw hemp fibers containing bioactive compounds (flavonoid). Featured with high efficiency, very short process time, less chemical and energy consumption, and high-quality fibers, this treatment method has a great potential for hemp cellulose fiber extraction.

Supplementary Information The online version contains supplementary material available at <https://doi.org/10.1007/s10570-023-05081-3>.

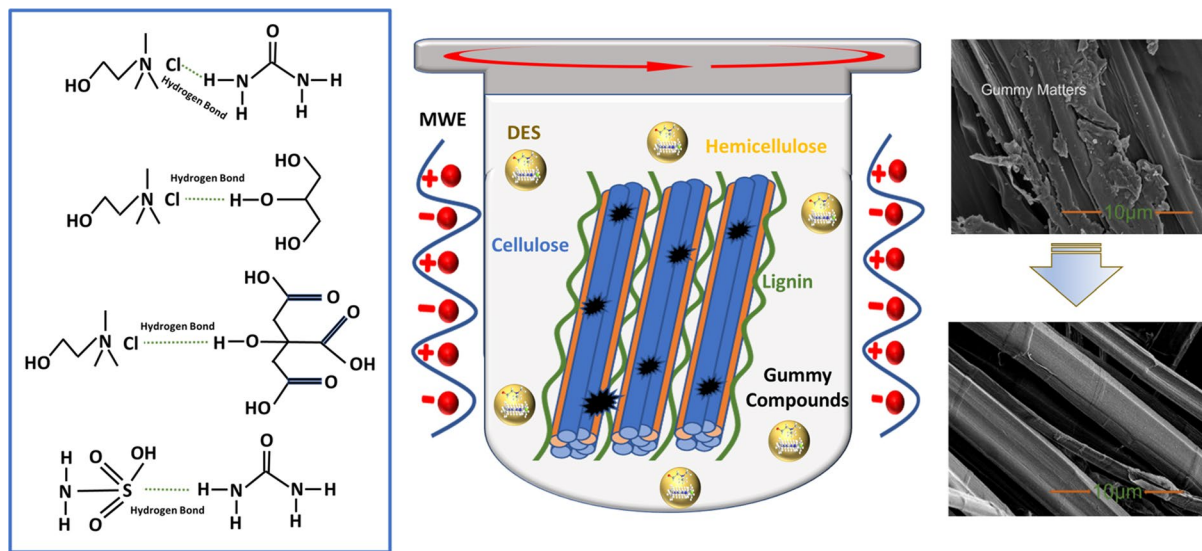
B. Ahmed · Q. Wu (✉)
School of Renewable Natural Resources, Louisiana State University AgCenter, Baton Rouge, Louisiana 70803, USA
e-mail: wuqing@lsu.edu

J. Gwon
Forest Products Department, National Institute of Forest Science, 57 Hoegiro, Dongdaemun-Gu, Seoul 02455, Korea

M. Thapaliya · A. Adhikari
School of Nutrition and Food Sciences, Louisiana State University AgCenter, Baton Rouge, LA 70803, USA

S. Ren
Institute of Urban and Rural Mining, Changzhou University, Changzhou 213164, China

Graphical abstract



Keywords Degumming · Cellulose · Deep eutectic solvent · Microwave heating

Introduction

Hemp is a promising biomaterial that has garnered great interest in recent decades as an alternative to other cellulosic fibers due to its biodegradability, fast-growing capability, and low production cost (Manaia et al. 2019). Hemp fibers have primarily been used in several industries such as textiles, composite, pulp and paper, and biorefinery. Hemp bast is mostly composed of cellulose, hemicellulose, lignin, and gummy compounds including pectin, oil, and wax. Lignin, a complex biopolymer consists of monolignols, including coniferyl alcohol, sinapyl alcohol, and *p*-coumaryl alcohol (Ralph et al. 2019). Gums consist of primarily proteins and resins (Soumya et al. 2019). The gummy compounds, hemicellulose, lignin, and other non-cellulosic components need to be removed from the fibers for subsequent textile processing, composite manufacturing, and biofuel preparation. Therefore, effective utilization of hemp fibers highly hinges upon efficient and successful degumming processes.

The degumming (or pretreatment) process in the textile industry includes alkali, dilute acid, steam explosion, hydrothermal, and enzymatic hydrolysis

methods (Subash and Muthiah 2021; Lyu et al. 2021; Mishra et al. 2021). Acid-base treatments of lignocellulosic biomaterials with the combination of oxidizing agents can remove intractable hemicellulose and lignin from the biomass structure. However, this widely used chemical treatment has suffered from several problems such as equipment corrosion, high energy input, and strong toxicity that causes serious environmental pollution (Murali et al. 2022). Enzymatic hydrolysis pretreatment is considered as an environmentally friendly pretreatment process. However, this process requires high energy consumption, prolonged process cycles, and suffers from the poor selection of apropos enzymes (Nogueira et al. 2021). In addition, organic solvent and biological treatment methods are widely used in the pulp industry. These methods also produced a high amount of wastewater, which needs to be retreated in the effluent plant, resulting in an increased production cost. Thus, all existing pretreatment methods cannot meet increased requirements to produce pure cellulosic fibers on an industrial scale with environmentally friendly features.

In recent years, ionic liquids (ILs) have emerged as effective solvents for various processes due to

their promising dissolution properties (Martins et al. 2022). However, the use of ILs is largely limited on the industrial scale because of their high toxicity and production cost. Additionally, the difficulties of the reuse and recyclability of ILs also limit the use of these solvents (Raza and Abu-Jdayil 2022). On the other hand, treatment with deep eutectic solvent (DES), one class of ILs, becomes one of the eco-friendly and viable pretreatment methods and provides an alternative to the traditional alkali-based chemical degumming treatment for natural fibers like hemp bast fibers. DESs are a potentially benign and inexpensive alternative to ILs (Abbott et al. 2004). DESs typically consist of a mixture of salt as a hydrogen bond acceptor (HBA) and a hydrogen bond donor (HBD). Quaternary ammonium salt has extensively been used as the HBA since it is inexpensive. A deep eutectic mixture possesses a much lower temperature than its individual components; thus, chemical reactions can be occurred at or near ambient temperature with these reagents (Smith et al. 2014). The dissolution properties of DESs owe to their ability of hydrogen bond formation as they can donate and accept protons and electrons. Several studies of DESs have been reported on the efficacy of delignification of various lignocellulosic biomass such as pine-wood, kenaf, ramie, wheat straw, and energy baggage (Bateni et al. 2017; Nie et al. 2020; Yu et al. 2019). Basic phenolic compounds such as p-hydroxyphenyl (H), guaiacyl (G), and syringyl (S) are connected predominantly by aryl ether bonds such as α -O-4 and β -O-4, or carbon–carbon bonds of the 5–5 or β – β types (Baruah et al. 2018). As a result, the lignin fractionation by DES depends primarily on the cleavage of carbon–carbon linkages (C–C bond) and aryl ether (C–O bond) in lignin, apart from breaking down the covalent bonds linking lignin–hemicellulose and hydrogen bonds linking lignin–cellulose. According to Lee et al. (2019), delignification of biomass with chlorine-based DES is based on the formation of hydrogen bonds between the chloride anions of DES and the carbonyl groups of lignin. Cl^- and other halogen anions may establish hydrogen bonds with lignin's OH groups, causing the lignin to dissolve and the aromatic compounds to be extracted. Because of this, the efficacy of delignification depends heavily on the DES capacity to establish H-bonds with lignin using electronegative halogen anion (Xu et al. 2020). DES with HBD having increased acidity and

proton-catalyzed bond breakage have both been identified as primary delignification mechanisms. For example, it was reported that oil palm empty fruit bunch pretreated with ChCl -lactic acid showed an enzymatic hydrolysis yield of 20.7% (Thi and Lee 2019).

The microwave energy (MWE)-assisted pretreatment process has already been proven as one of the promising pretreatment technologies due to the less process time consumption, easier control of chemical reactions, fast-heating, and low energy input with microwave radiation (Wang et al. 2020). The molecular polarity of DESs can be improved while their ionic character is maximized by microwave irradiation, and thus, biomass pretreatment temperature and time might be reduced (Tan et al. 2020). It has been reported that MWE pretreatment combined with other chemical reagents is an effective delignification process than that of the conventional heating for the rice straw (Hartati et al. 2021; Li et al. 2019; Sorn et al. 2019). Liu et al. (2017) reported that a combined MWE-DES (DES made of choline chloride and oxalic acid dihydrate) treatment for 3 min at 80 °C was able to cleave the lignin–carbohydrate complexes and an ultrafast fractionation of wood lignocellulose (poplar wood) occurred. Chen and Wan (2018) also found that the synergistic effect of combined MWE-DES (DES made of choline chloride and lactic acid) treatment for only 45 s at 152 °C was capable of fractioning the lignocellulosic biomasses (corn stover, switchgrass, and *Miscanthus*). About 37.5% lignin removal was observed with a 30 min combined microwave and DES (made of choline chloride and formic acid) treatment of rice husk. However, it required 2 h of DES treatment at 155 °C for the conventional heating system to get that comparable lignin removal performance (about 46.8%) (Kumar et al. 2019). Thus, a combined MWE-DES pretreatment was more efficient and utilized less energy than conductive heating to process biomass. Therefore, combined microwave and DES treatment can be an effective and eco-friendly pretreatment method for lignocellulosic biomaterials. In our previous study, MWE-DES treatment (DES made of choline chloride and urea) was applied to hemp fibers at 120 °C for 90 min, yielding a holocellulose content of 98.63% (Ahmed et al. 2022). Results also revealed that the hemp fiber surface underwent structural change during the

treatment and the fibers showed improved ultraviolet (UV) resistance and thermal stability. The study, however, is limited to one DES system with few treatment conditions. Henceforth, it is essential to study the efficacy of other DESs in terms of lignin removal, and various reaction parameters such as treatment time, and MWE-DES reaction temperature. The suitability of DES constituents (hydrogen bond acceptors and donors) in relation to stable DES formation, treatment effectiveness, and DES eco-friendliness for pure cellulose extraction is also needed to be further demonstrated.

This work aimed to contrast several DES systems for the degumming of hemp fibers in comparison with traditional alkali and acid-based treatment processes on process efficiency and fiber quality. Particularly, four DES systems, one alkali, and one acid process with and without combined MWE heating were used to degum the hemp fibers. After degumming, treated hemp fibers (mainly cellulose) were characterized using several advanced analytical techniques and antibacterial testing. Experiments reveal that this MWE-DES pretreatment is a cost-effective, environmentally beneficial, and logically practicable way of degumming hemp bast fibers and utilizing fiber materials in their entirety.

Experimental section

Materials

Raw hemp bast fibers that had been mechanically separated from the entire hemp stalk were purchased in large quantities from a commercial source. The fibers contained a small amount hurd material randomly distributed in the system. Glycerol, sulfamic acid,

citric acid, and sodium sulfide were purchased from VWR Life Science in ACS reagent grade (Solon, Ohio, USA). Purity greater than 98% choline chloride (CC) was obtained from TCI America (Portland, OR, USA), crystallized urea (U) from VWR BDH Chemicals (Radnor, PA, USA), ACS-grade sodium hydroxide (NaOH) from Fisher Chemical (Fair Lawn, NJ, USA), and ACS reagent grade hydrogen peroxide (30% aqueous solution) from J.T. Baker (Radnor, PA, USA).

Degumming process

Raw hemp fibers were first cleaned manually using a small lab-scale carding machine to remove hurd from the fibers. The cleaned hemp fibers were stored in the laboratory at room condition for further processing. Table 1 lists the degumming methods used for the study.

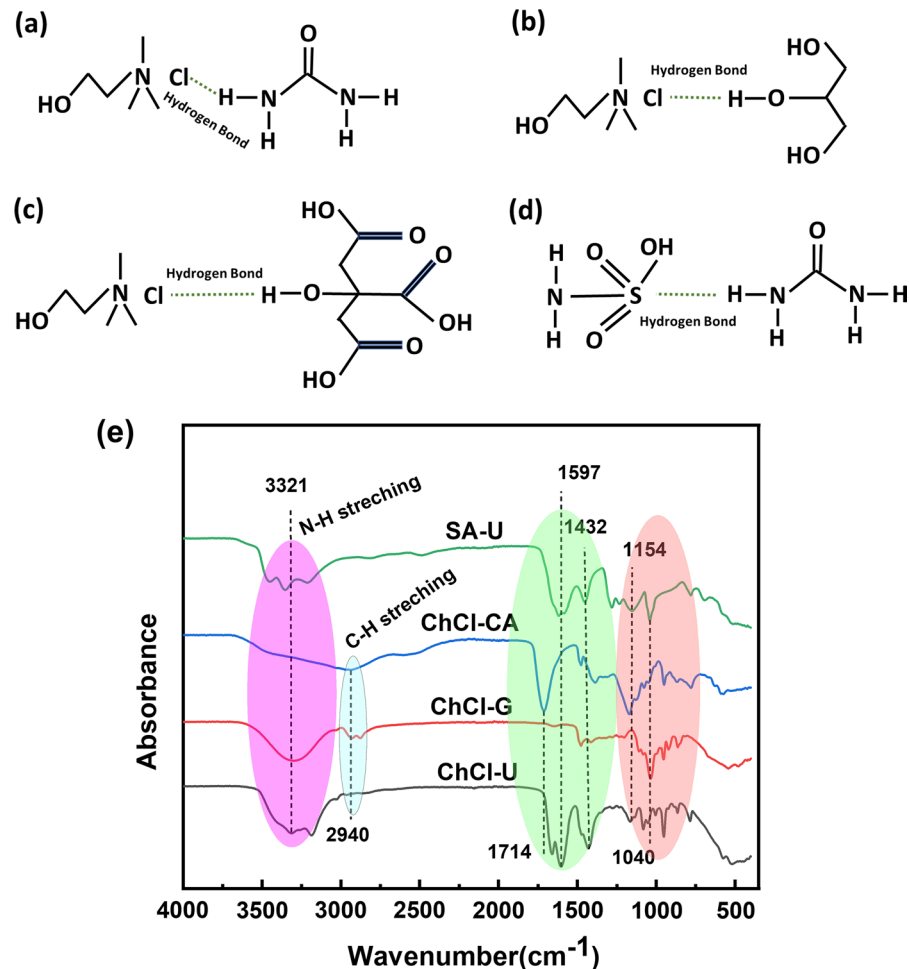
System A represents untreated control hemp bast fibers. System B was a traditional kraft pulping process with 12% active alkali and 25% sulfidity (addition of NaOH and Na₂S acted as Na₂O) and a solid–liquid ratio of 1:8 (v/w) in a sealed oil bath for 3 h at 160 °C. Bleached hemp kraft fibers from treated fibers were obtained using an alkaline peroxide treatment (2% NaOH and 4% H₂O₂) at 90 °C for 1 h in an oil bath. Bleached fibers were washed with tap water to achieve neutrality and oven-dried at 60 °C.

System C to System F was based on four different types of DES systems in combination with MWE heating (Table 1 and Fig. 1). Choline chloride (C, D, E) and sulfamic acid (F) were used as hydrogen bond acceptors (HBA), and urea (C and F), glycerol (D), and citric acid (E) were used as hydrogen bond donors (HBD). All the DESs were obtained from

Table 1 Summary of treatment conditions for the production of hemp cellulose fibers

ID	Sample type	Process	Chemicals	Fiber/chemical ratio	Heating method
A	Raw	Raw	None	None	None
B	Kraft	Alkali	NaOH and Na ₂ S	1:8	Oil Bath: 3 h at 160 °C
C	ChCl-U	DES	Alkaline peroxide	1:10	Oil Bath: 1 h at 90 °C
D	ChCl-G	DES	Choline chloride-urea	1:10	MWE:5 min at 100 °C
E	ChCl-CA	DES	Choline chloride-glycerol	1:10	MWE:5 min at 100 °C
F	SA-U	DES	Choline chloride-citric acid	1:10	MWE:5 min at 100 °C
G	Sul-M	Acid	Sulfamic acid-urea	1:6.18	MWE:5 min at 100 °C

Fig. 1 Schematic showing reaction mechanism and FT-IR spectra of different DES systems **a** choline chloride and urea **b** choline chloride and glycerol **c** choline chloride and citric acid **d** sulfamic acid and urea, and **e** FT-IR spectra of all the DES systems



the mixture of HBA and HBD at a molar ratio of 1:2. Until a homogenous solution was achieved, the mixture was heated at 80–90 °C for 1–2 h in an oil bath. The DES solution was added to the 90 ml Teflon vessel containing the clean hemp fiber samples. For the degumming process of hemp fiber samples, an Ethos X microwave extraction system (Milestone Inc, Shelton, CT, USA) was employed with a 1:10 fiber-DES ratio (heating at 100 °C for 5 min). The microwave extraction system has a power output of 1000 kW and a stirring efficiency of 24%. After degumming, treated fibers were washed with tap water and oven-dried at 60 °C, and stored for further characterization.

System G was an acid based MWE treating method (Huang 2018). The process was carried out with 2 g raw hemp fibers, methanol (12 g), and

sulfuric acid (0.36 g), well mixed in a test vessel. A typical microwave run was carried out for 5 min at 160 °C using the same microwave extraction system (Ethos X, Milestone Inc, Shelton, CT, USA). The reaction was quenched in an iced bath and the solid fibers were washed with tap water. The fibers were dried in an oven at 60 °C and stored for further characterization.

Characterization

Scanning electron microscopy (SEM)

The surface morphology and cross-section of hemp fibers were investigated by using an electron microscope (Model: JSM-6610 LV SEM, JEOL, Japan)

in a high vacuum condition at an accelerated voltage of 5 kV and an emission current of 24 pA. Fiber samples were cut into small pieces and coated with an EMS550X sputter coater machine before scanning. For cross-section imaging, ion beam milling was used for preparing samples for SEM analysis. During this process, the fiber was bombarded with a high-energy argon-ion beam to achieve high quality cross-section surface whilst minimizing deformation or damage to the fibers.

Fourier transform infrared (FTIR) analysis

FTIR scanning was done to identify the functional groups of both treated and pristine hemp fibers, and DESs. The formation of hydrogen bond in the DESs system was also analyzed using FTIR spectra. The prepared DESs solution were directly scanned without further sample preparation to obtain FTIR spectra. FTIR spectra of treated and untreated fibers, and DESs solution were taken at a resolution of 4 cm^{-1} , 32 scans per sample, and with a $400\text{--}4000\text{ cm}^{-1}$ wavelength range by using a Bruker Alpha FTIR spectrophotometer (Ettlingen, Baden-Württemberg, Germany).

X-ray diffraction (XRD) analysis

A PANalytical Empyrean X-ray Diffractometer (Malvern, Malvern Worcestershire, UK) was used to collect XRD spectra of both treated and raw hemp fibers. The equipment is equipped with a Pixel-3 detector a $\text{CuK}\alpha$ radiation source ($\lambda=0.15418\text{ nm}$) at 45 kV and 40 mA. To correct the background, a blank run was done (run without sample) and the data was subtracted from the observed data with test samples. The crystallinity index (derived from normalized XRD spectra) of both treated and raw hemp fibers was determined using the Segal equation (Segal et al. 1959).

$$\text{CrI\%} = \frac{I_{200} - I_{\text{am}}}{I_{200}} \times 100\% \quad (1)$$

where I_{200} is the highest intensity at 22.6° corresponding to the crystalline cellulose and I_{am} is the minimum intensity at roughly 18° relating to the amorphous regions of the cellulose.

Chemical structure analysis

The solid-state NMR test of both untreated and treated hemp fibers was performed on a 3-channel Bruker AV-400 (Bruker BioSpin, Billerica, MA, USA) equipped with a 400 MHz spectrophotometer. The following parameters were used for one-directional (1D) cross-polarization magic angle (CP/MAS ^{13}C NMR): MAS rate-10 kHz, 4096 Scans, relaxation delay-2 s, and CP contact time-2 ms. NMR data were examined and processed using the Topspin Software (Bruker, version-2.1) and Origin Pro (2021 version).

Chemical composition analysis

According to the American Society for Testing and Materials (ASTM) standard (D-1105-96), extractive-free samples were prepared from untreated raw and treated hemp fibers using the Soxhlet extraction method with a slight modification as reported in the literature (Jung et al. 2015). The solvent for the extraction was made of water and ethanol-toluene (1:2 v/v). 3 g hemp powder fiber samples were placed in the thimble paper of the Soxhlet apparatus, and the extraction solvent was incubated for 4 h. The sample was then filtered, and the excess solvent was removed using Buchner funnel-assisted vacuum filtration. Toluene was cleaned from the sample and thimble paper by washing with ethanol. The sample was transferred to the Soxhlet apparatus for ethanol extraction for 4–5 h until the ethanol became colorless in the siphon. The sample was removed from the thimble paper and air-dried to get an alcohol-free sample. The Soxhlet extraction was repeated using deionized water, filtered, and washed with deionized water. Then the sample was oven-dried at 100°C .

Holocellulose was obtained from extract-free hemp fiber samples using a delignification treatment reported in the literature (Jung et al. 2015). Extractive-free hemp sample (500 mg) was added to a solution of 200 mg sodium chlorite and 30 ml water. Then the mixture was adjusted to a pH of 3.5 by adding 10% acetic acid and heated at 85°C for 30 min. Then the sample was filtered and washed with distilled water and oven-dried at 100°C . This oven-dried sample is considered as holocellulose. Cellulose and hemicellulose content in the holocellulose were determined

according to the KSM 7044 standard—testing method for alpha, beta, and gamma cellulose in pulp as reported in the literature (Jung et al. 2015). Holocellulose sample (300 mg) was added to the 3 ml water-sodium hydroxide solution (17.5 wt% sodium hydroxide) and stirred magnetically at room temperature for 20 min. After stirring, the mixture was left standstill for another 5 min and vacuum filtered and rinsed with distilled water. Then the sample was oven-dried at 100 °C to the constant weight and considered as cellulose content in the holocellulose sample. Hemicellulose content was determined by subtracting cellulose weight from the holocellulose weight.

The lignin content of both untreated and treated hemp fibers was determined using a slightly modified TAPPI technique similar to the one reported in the previous work (Liu et al. 2020). A 20 ml vial was filled with 0.1 g hemp fiber sample and 1.5 ml of aqueous H₂SO₄ (72%) solution. The mixture was then swirled for 2 h at room temperature. After stirring the mixture, 56 ml deionized water was added, and the solution was placed in a 250 ml rounded bottom flask. After 4 h of refluxing at 100 °C, the suspension was filtered, and the solid residue was dried in an oven at 60 °C for 24 h. The acid-insoluble lignin was extracted from the solid residue and quantified gravimetrically. 100 ml of deionized water was used to dilute the filtrate. A UV-vis spectrophotometer (ThermoFisher Scientific Inc. Waltham, MA, USA) at 205 nm and an extinction coefficient of 110 Lg⁻¹ cm⁻¹ was used to detect acid-soluble lignin from the diluted filtrate.

Thermal stability analysis

Thermogravimetric (TG) analysis of both untreated and treated hemp fibers was performed using a TG analyzer (Model-Q50, TA Instruments Inc. New Castle, DE, USA) in a nitrogen atmosphere with a flow rate of 40 ml/min. The heating was maintained at a rate of 10 °C/min to 540 °C. All TG samples were about 5 mg in weight. TG and derivative TG thermograms were obtained as a function of weight and temperature to investigate the thermal degradation process of the hemp fibers.

Antibacterial Testing

The hemp fibers (both treated and raw hemp fibers) were tested for their antibacterial activity against

E. coli (ATCC25922). The bacterial culture was maintained in the nutrient agar slopes and grown in tryptic soy broth and incubated for 18 h at 37 °C. A sterilized buffer solution of 0.3 M KH₂PO₄ was used to prepare the working bacterial dilution. An absorbance of 0.28 ± 0.02 at 475 nm of bacterial dilution is regarded as a concentration of 1.5–3.0 × 10⁸ colony-forming units per milliliter (CFU/mL). All the sterilization and media preparation were performed using an autoclave at 121 °C for 20 min. The antibacterial activity of hemp fibers was analyzed according to the ASTM E2149-20 method. Powdered hemp fibers were obtained using a milling machine. 1 g of the powdered hemp fiber was added to a 250 ml flask containing 50 ml of bacterial dilution. The flask was then agitated for 1 h at 250 rpm at 25 °C using an agitation shaker. 1 ml of the solution was inoculated on a Petri plate containing 15–20 ml of tryptic soy agar after shaking. Three replicates were utilized for each fiber type. All infested plates were grown for 24 h at 37 °C. Active bacteria were enumerated after culture, and the anti-bacterial effect was assessed. After a defined contact period, the percentage decrease of bacterial organisms in treated samples compared to "inoculum alone" samples is measured. The following percentage reductions were obtained by counting CFU/mL of bacteria:

$$\text{Reduction}(\%) = \frac{N_{\text{control}} - N_{\text{sample}}}{N_{\text{control}}} \times 100\% \quad (2)$$

where $\text{Reduction}(\%)$ = Bacterial colony reduction%, N_{control} = Bacterial colony numbers on the control plate, and N_{sample} = Bacterial colony numbers on the inoculated plate of the sample.

Flavonoid structure analysis

The presence of the flavonoid structure in the hemp fiber extract was studied as described in the previous study (Cui et al. 2021). 5 g raw hemp fibers were immersed in 75% (weight/weight) ethanol and refluxed at 100 °C for 3–5 h. The filtrate was the hemp extract. The flavonoid structure was analyzed using a Bruker Alpha FTIR spectrophotometer (Ettlingen, Baden-Württemberg, Germany) and a UV-vis spectrophotometer (ThermoFisher Scientific Inc. Waltham, MA, USA).

Results and discussion

DES characteristics

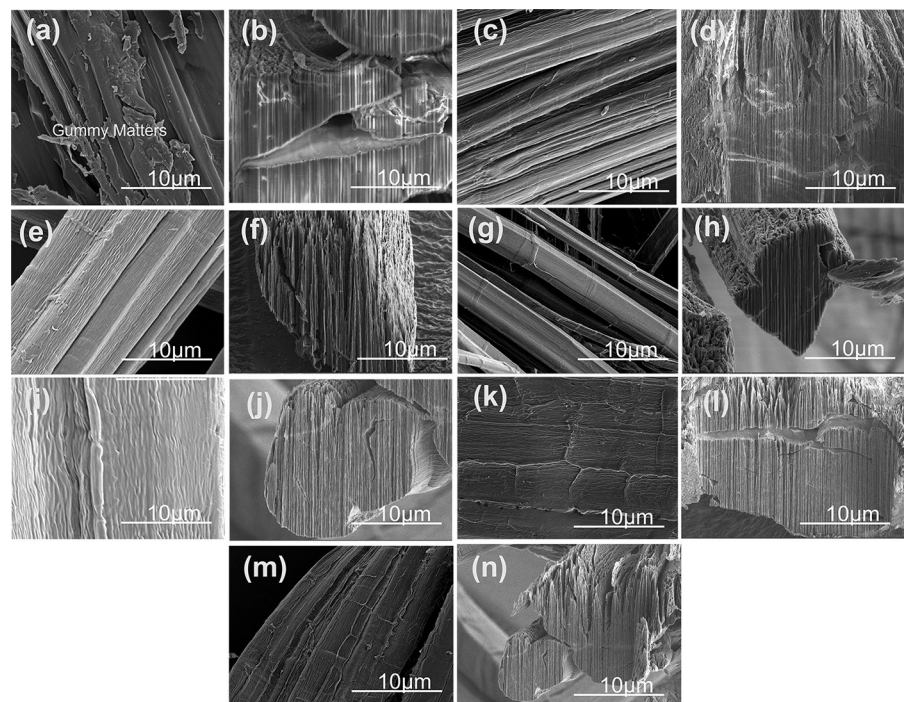
The reaction mechanisms of DESs are shown in Figs. 1a to d for different systems. The corresponding FTIR spectra of the DES systems presented in Fig. 1e revealed the chemical structure and hydrogen bond interactions between HBD and HBA. The symmetric and asymmetric stretching of the alkyl chain (CH_2 vibration) was observed at the band of 2940 cm^{-1} . A broad peak of the N–H phase and NH_2 stretching at 3321 cm^{-1} of the DESs confirmed hydrogen bond between HBA and HBD (Stefanovic et al. 2017). The symmetric and asymmetric C–H vibrations of CH_3 moiety were assigned to the peak at 1432 cm^{-1} . Those stretching appeared as a broad peak in all the DES systems (except ChCl-CA). The peaks at the region of $1040\text{--}1154\text{ cm}^{-1}$ were attributed to the C–C stretching of DESs (made of choline chloride-citric acid and choline chloride-glycerol) and symmetric C–N bending of the DESs (made of choline chloride-urea and sulfamic acid-urea). Symmetric NH_2 and N–H bending were noticed at a wavenumber range of

$1597\text{--}1714\text{ cm}^{-1}$. Therefore, a successful hydrogen bond network was formed in the DES systems.

Longitudinal and cross-section morphology

The degumming effect of hemp fibers was revealed by the longitudinal and cross-section views of raw and treated hemp fibers as shown in Fig. 2. Raw hemp fibers (Fig. 2a – longitudinal view) contained significant gummy compounds. However, the surface structure of the hemp fibers was changed after the degumming treatment. The MWE-DES treatment (Figs. 2e, g, i, and k) led to smooth fiber surface treatment (comparable with the fibers of the traditional kraft treatment) (Fig. 2c). MWE-DES treatment not only removed the gummy matters but also preserved the inherent celullosic structure of the fibers as shown in Figs. 2e to 2l. However, the traditional kraft fibers (Fig. 2c) and hydrolyzed (half-esterified) fibers (using sulfuric acid and methanol- Fig. 2m) had a few cracks and voids. Hence, these treatments are considered as harsh treatment, affecting the physical and mechanical properties of the hemp fibers. On the other hand, the MWE-DES treatment produced individual hemp fibers with a clean fiber structure (Figs. 2e–l), suggesting the

Fig. 2 SEM pictures of raw and treated hemp fibers and their cross-sections: **a, b** sample A (Raw), **c, d** sample B (bleached Kraft), **e, f** sample C (ChCl-U), **g, h** sample D (ChCl-G), **i, j** sample E (ChCl-CA), **k, l** sample F (SA-U), and **m, n** sample G (Sul-M)



removal of gummy materials and impurities without damaging the fibers.

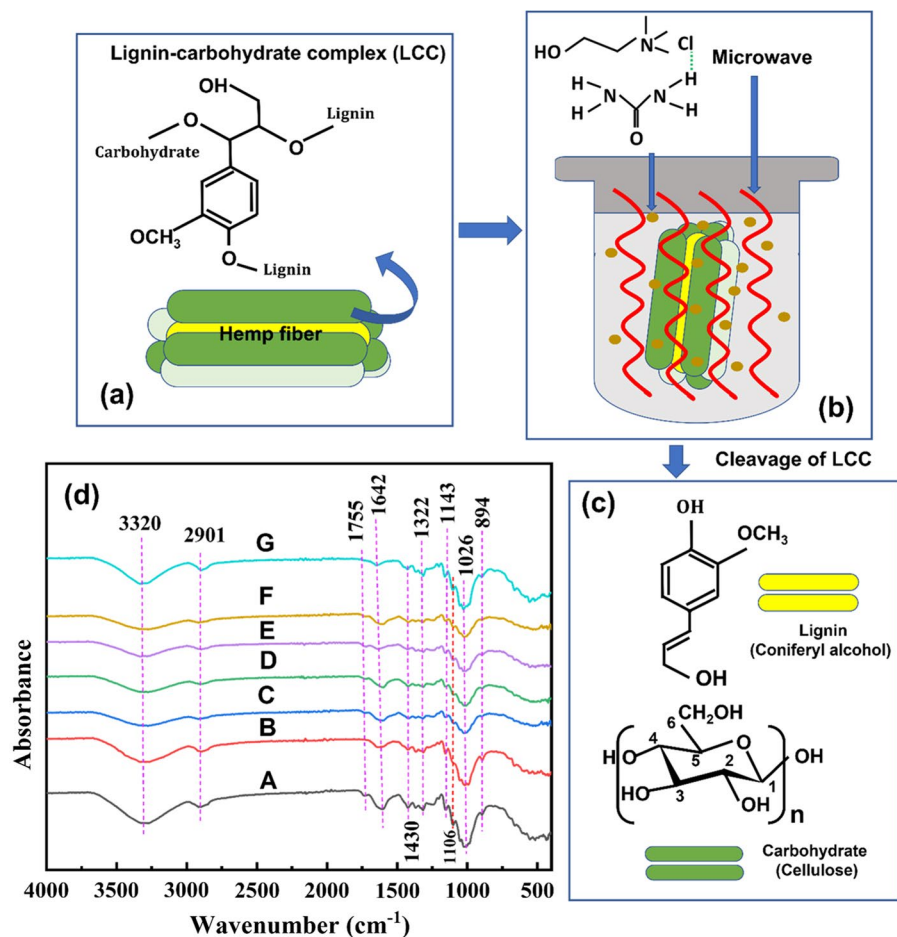
Cell walls of a single fiber are composed of a sequence of helically coiled cellular microfibrils from cellulose molecules that are arranged hierarchically with lignin bonding between the fibrils (Liu et al. 2015). They also had various cross-section shapes, and these variations were correlated to the number of fibers in each region. Regardless of whether the fibers were treated or not, they both had a pentagonal cross-sectional shape (Fig. 2b, d, f, h, j, l, and n). Weak intermolecular hydrogen bonds and lignin, pectin, and other gummy substances held the elementary fibers of the raw hemp fiber bundles depicted in Fig. 2b together. Raw hemp fibers' cross-sectional image showed that gummy compounds were strongly cemented to each of the cells in the fiber structure

(Fig. 2b). Clean fiber surfaces in the MWE-DES treated fibers (Figs. 2e, g, i, and k) suggested successful delignification. A swelled fiber bundle can be seen in the cross-section of alkalized (Fig. 2d) and partially acid-hydrolyzed fibers (Fig. 2n). Figures 2f, h, j, and l showed that fibers treated with MWE-DES had a more uniform geometry and a trend toward single-fiber openness, indicating that gummy compounds were removed from the fiber structure.

Fiber surface chemical structure

The FTIR spectra were obtained to analyze the chemical structure changes and to identify the interaction of functional groups between fibers and DES. The peak at 894 cm^{-1} band confirmed the presence of β -1,4 glycosidic linkages, meaning that the

Fig. 3 **a–c** A schematic of LCC cleavage (benzyl ether linkage) using MWE-DES (ChCl-U) treatment of hemp fibers **d** FTIR spectra of both untreated and treated hemp fibers



cellulose structure of MWE-DES treated fibers was intact (Vârban et al. 2021). The band at 1430 cm^{-1} was assigned to the ester bond of hemicellulose (Fig. 3d). This peak was stretched and straightened in the MWE-DES-treated fibers, suggesting the removal of amorphous cellulose and hemicellulose from the treated fiber structure. In addition, the symmetric and asymmetric stretching of methylene groups (CH_2) in alkyl chains were attributed to the band at 2901 cm^{-1} (C-H stretching), indicating the presence of waxes and impurities in the raw hemp fibers. However, this peak was broadened and stretched in the treated fibers, indicating the removal of impurities from the treated fibers. Carbon–carbon (C–C) ring stretching of lignin structure found in the untreated raw and treated fibers at 1143 cm^{-1} band that was reduced and disappeared from the MWE-DES treated fibers, suggesting the removal of lignin from the fiber surface. In the raw hemp fibers, the peak at the 1755 cm^{-1} band was assigned to the ester and carbonyl groups of hemicellulose and pectin. This peak disappeared from the MWE-DES treated fibers, indicating the removal of pectin and hemicellulose from the fiber structures. Functional group assignment of FT-IR spectra for raw and treated fibers was presented in Table S1. Figure 3b shows a typical fiber-DES reaction during MWE-DES treatment (ChCl-U).

Fiber crystallinity

X-ray diffraction patterns were obtained for the raw and degummed hemp fibers depicted in Fig. 4a. All the treated and untreated fibers showed a typical crystalline peak between 22° and 23° , which

corresponded to the crystallographic plane (200) of cellulose I. The peaks at 14.6° and 16.4° , and 34.8° at the crystallographic plane of 110 , 110 , and 004 , respectively, corresponded to cellulose I (French 2014). Additionally, Fig. 4a clearly shows a small peak at about 12° position and an enhanced peak at about 20° position, indicating a certain amount of cellulose II (French 2014). Henceforth, the high (110 plane) peak of cellulose II in the XRD pattern of the sample B had tails that overlap the amorphous 18° point and increased the intensity for the amorphous measurement. Therefore, the calculated crystallinity index% using the Segal method cannot be appropriately applied with the mixed composition of cellulose I and II. However, as shown in Fig. 4b, raw hemp fibers had a crystallinity index of 76.09%, which was the lowest as compared to that of all the treated fibers. The highest crystallinity index (84.4%) was obtained from the MWE liquefied fibers (sample Sul-M) due to the occurrence of acid hydrolysis and crystal orientation of the fibers, suggesting the removal of amorphous cellulose, hemicellulose, and gummy materials. All the MWE-DES treated fibers exhibited a comparable crystallinity index with the MWE liquefied and kraft fibers. The higher crystallinity index of MWE-DES treated fibers indicated the removal of gummy compounds from the fiber structure. The combined effect of the protonation of DES and uniform distribution of microwave energy might be the result of breaking ether and ester linkage of the lignin-carbohydrate complex in the fiber structures, suggesting the packing of cellulosic chains. Hence, the enhanced crystal orientation was obtained in the MWE-DES treated fibers, which in turn, produced a higher crystallinity index that was comparable with

Fig. 4 XRD patterns of both treated and raw hemp fibers **b** crystallinity index% of raw and degummed hemp fibers

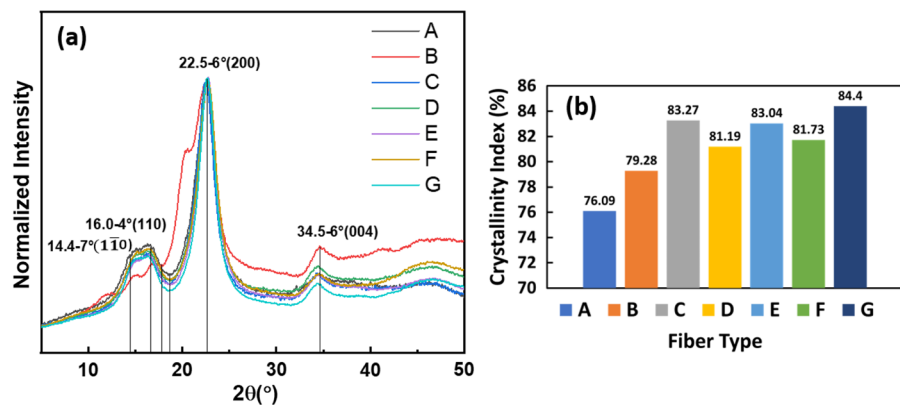
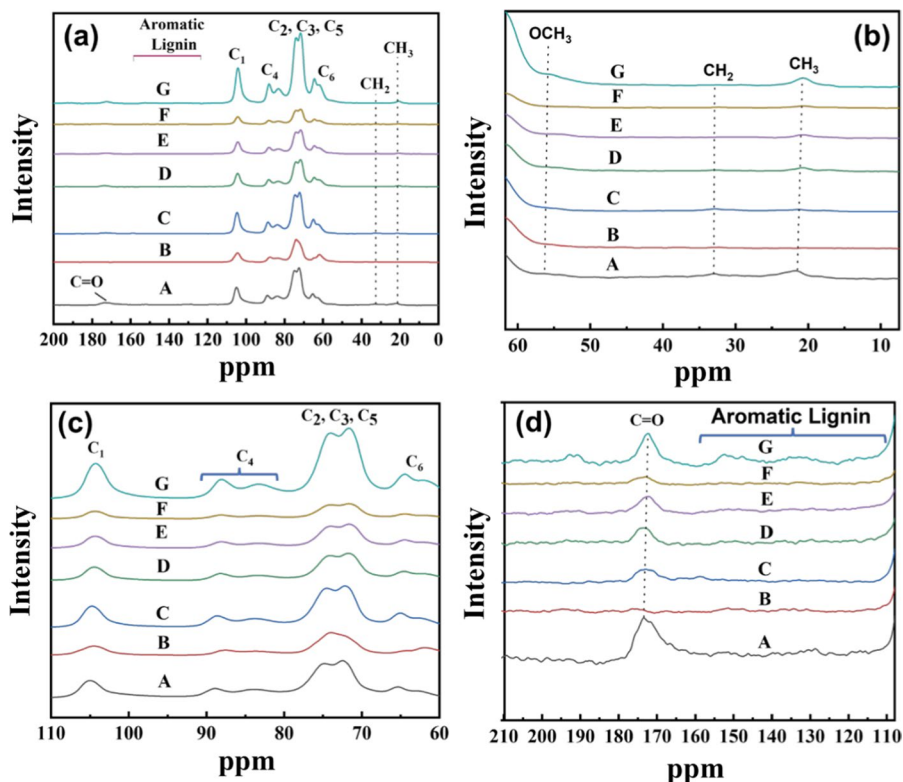


Fig. 5 The chemical shift of CP-MAS/ ^{13}C -NMR spectra of both raw and treated fibers at different ppm levels (a–d)



the increased crystallinity index of alkali (NaOH) treated hemp fibers reported from previously published studies (Behera et al. 2021; Ghosh et al. 2020; Tanasă et al. 2020; Viscusi et al. 2020). In addition, the degradation of hemicellulose macromolecules liberates the pectin and other molecules of gummy compounds such as oil and wax. The liberation of the molecules of gummy compounds was facilitated by microwave radiation as the radiations were uniformly dispersed throughout the fiber structure; therefore, a good degumming effect was obtained in the MWE-DES treated fibers which was also supported by the SEM images.

Fiber chemical structure

The obtained CPMAS ^{13}C NMR spectra as shown in Fig. 5a–d revealed the chemical structural compositions of the raw and degummed hemp fibers. Table S2 presents the.

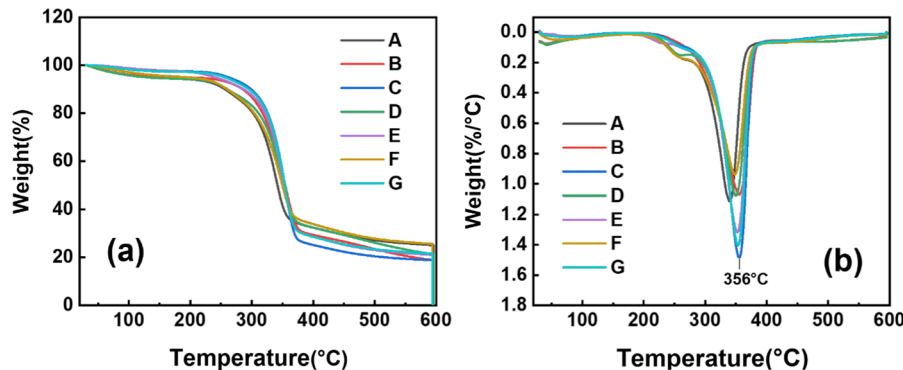
assignment of the NMR band at different ppm levels. A notable change in NMR spectra was observed in the degummed hemp fibers. The two main regions

of NMR spectra at 110–160 ppm and 10–110 ppm were assigned to the signal of aromatic lignin structures and carbohydrate complexes (mainly cellulose and hemicellulose), respectively. The carbohydrate complex region provided intense and overlapped peaks due to the agglomeration and structural similarities of cellulose and hemicellulose. The most intense peaks at 68–80 ppm were the C_2 atom of cellulose carbons. In addition, the chemical shift of less ordered C_4 and C_6 carbons of crystalline and amorphous cellulose was attributed to the regions of 80–90 ppm and 63–67 ppm, respectively. Guaiacyl and syringyl moieties related to the methoxy groups of lignin structure were also observed in the region of 55–59 ppm (Kostryukov et al. 2021). The chemical shift of the carbonyl carbon of the lignin was observed at around 174 ppm in the raw hemp fibers. However, this peak almost disappeared in the MWE-DES-treated fibers, indicating the removal of lignin. A broad peak was observed in the 21 ppm and 34 ppm in the raw hemp fibers, these are the methyl and methylene carbons of lignin. These peaks also disappeared in the

Table 2 Comparison data of the chemical composition of untreated and treated hemp fibers (C. = Cellulose, H.C. = Hemicellulose, H.O. = Holocellulose and others, A.I.L = Acid insoluble lignin, A.S.L. = Acid soluble lignin, and Total L. = Total lignin)

System ID/sample type	KSM 7044		TAPPI method				References
	C. (%)	H.C. (%)	H.O. (%)	A.I.L. (%)	A.S.L. (%)	Total L. (%)	
A: Raw	66.03	13.47	81.60	12.1	6.30	18.4	This study
B: Kraft	92.11	3.69	97.80	1.30	0.90	2.20	
C: ChCl-U	87.40	6.72	97.12	1.91	0.97	2.88	
D: ChCl-G	84.91	9.13	97.04	1.87	1.09	2.96	
E: ChCl-CA	82.26	10.12	96.38	2.31	1.31	3.62	
F:SA-U	80.63	11.55	95.18	3.03	1.79	4.82	
G: Sul-M	85.72	6.51	97.71	1.40	0.89	2.29	
18 wt% NaOH						~2.44	Kostic et al. (2008)
17 wt% NaOH						3.09	Kostic et al. (2010)
1 M NaOH						~4.50	Mijas et al. (2021)
0.7 wt% NaClO ₂						3.09	Pejic et al. (2008)
10 wt% NaOH						2.65	Kabir et al. (2013)

Fig. 6 TG and DTG curves of both untreated and treated hemp fibers



MWE-DES treated fibers, suggesting the removal of lignin from the fiber structure.

Fiber chemical composition

The cellulose, hemicellulose, and residual lignin content of the untreated and treated fibers are listed in Table 2. As shown in Table 2, different treatment methods significantly affected the chemical compositions of the fibers. The residual lignin content of the raw hemp fibers (sample Raw) was 18.4%. The lowest lignin content of 2.2% was found in the krafted fiber. However, DESs made of choline chloride, urea, and glycerol (sample ChCl-U and sample ChCl-G) yielded a lower residual lignin content as compared to these of other DES-treated fibers. However, the comparable residual lignin content of the DES-treated

fibers with traditional kraft fibers indicated that DESs were able to remove most of the gummy compounds from the fiber structure, which in turn, contributed to the increased cellulose content in the treated fibers.

Thermal stability

Figure 6 shows the measured TG and DTG curves of the hemp fibers. The thermal degradation process of hemp fibers is divided into mainly three stages such as moisture and chemical bond water evaporation at 50–150 °C, hemicellulose degradation at 220–300 °C, and pyrolysis of cellulose at 300–400 °C. However, the decomposition of lignin in the natural fibers was started at 280 °C and ended up at 550 °C (Ahmed 2021). The thermal degradation

Table 3 TG data of both untreated and treated hemp fibers

Sample type	Weight loss (%)			Onset temperature (°C)	Max weight loss rate temperature T_{\max} (°C)	Residue weight (%)
	50–150 (°C)	220–300 (°C)	300–400 (°C)			
A	3.68	12.60	47.18	306.30	338	26.76
B	3.35	7.70	55.57	314.92	355	21.31
C	1.99	6.94	62.95	325.18	356	21.10
D	3.76	10.29	49.24	314.30	351	23.63
E	1.97	8.47	57.88	322.85	353	22.74
F	3.59	12.13	45.83	308.65	348	28.54
G	2.23	7.34	59.05	323.79	353	23.67

event of lignin occurred at an extended range of temperatures due to its complex phenolic structure. The pyrolysis of cellulose includes depolymerization, molecular chain breaks, and dehydration of glyco-groups. The lowest weight losses of 1.99% and 1.97% were observed in ChCl-U and ChCl-CA samples at the first thermal event of 50–150 °C, indicating the reduction of hydroxyl groups from the MWE-DES treated fiber structure. The maximum weight loss from the DTG curve of the ChCl-U sample was 62.95% at 356 °C (designated T_{\max}), and this temperature fell under the cellulose degradation event. Additionally, the main weight loss at the first DTG curve was shifted toward a higher temperature (i.e., T_{\max} of sample Raw = 338 °C, and MWE-DES treated samples = 348 °C), suggesting the higher thermal stability of the treated fibers. An increased crystallinity leads to higher thermal stability due to better molecular arrangement and packing of cellulosic chains. Therefore, the higher crystallinity index obtained from the XRD data also confirmed the higher thermal stability of the MWE-DES treated fibers (Table 3).

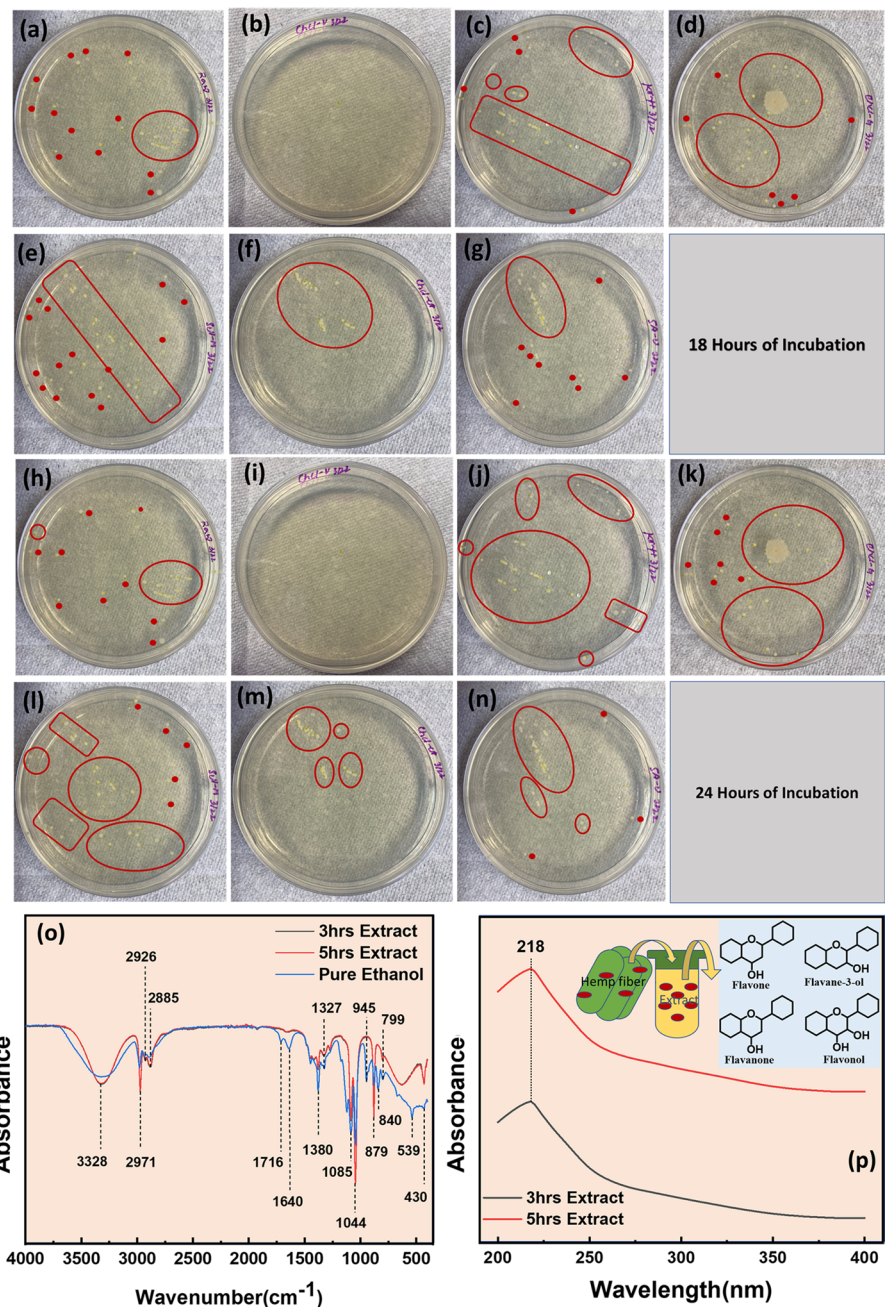
The maximum mass loss was concentrated at 300–400 °C because of the highest amount of cellulose exposure during this thermal event. Therefore, the composition of cellulose in the MWE-DES treated fibers was higher than that of raw hemp fibers, suggesting the removal of gummy and non-cellulosic compounds. For the second stage of thermal degradation (220–300 °C), the rate of weight loss was low for the MWE-DES treated fibers, this was also an indication of the removal of hemicellulose. The highest char content of 26% was recorded for raw hemp fibers (sample Raw) and the weight loss at the main degradation stage of lignin (at 400–550 °C) was very

low in the MWE-DES treated fibers as compared to the raw fibers, indicating that DESs can effectively remove lignin from the fiber structure.

Bacterial growth inhibition

Figure 7 and Table 4 show the antibacterial activity of both raw and degummed hemp fibers. It was evident that MWE-DES treated fibers showed an excellent inhibition of *E. coli* growth (Table 4). The hemp fibers exhibit antibacterial activity due to the presence of inherent chemical components such as alkaloids, flavones, and saponins (Iseppi et al. 2019). The removal of gummy compounds might increase the reactivity of these compounds. The control fiber plate (Fig. 7a, h) had about 15 colonies while all the MWE-DES treated fibers had bacterial colonies of 26 or less. Therefore, it was assumed that all the treated fibers showed similar bacterial growth inhibition with the untreated (sample Raw) fibers. However, the bacterial growth reduction for the alkalinized fibers (Fig. 7c, j) and acid-hydrolyzed fibers (Fig. 7g, n) were 6 and –173%, respectively. Additionally, DES (ChCl-U) treated fibers (Fig. 7b, i) were fully resistant to bacterial growth for both 18 h and 24 h cultivation. MWE-DES treatment of hemp fibers removed mostly gummy compounds (pectin and wax), lignin, amorphous cellulose, and hemicellulose. These compounds, rich in hydroxyl groups, were removed from the fiber structure after MWE-DES treatment. In addition, OH groups of the free water and bond water molecules in the hemp fiber structure were also reduced due to the MWE-DES degumming treatment. Therefore, increased hydrophobicity might be

Fig. 7 Antibacterial activity of both raw and degummed hemp fibers. **a** and **h** sample A (raw), **c** and **j** sample B (kraft), **b** and **i** Sample C (ChCl-U), **d** and **k** sample D (ChCl-G), **e** and **l** sample E (ChCl-CA), **f** and **m** sample F (SA-U), **g** and **n** sample G (Sul-M), **o** FTIR spectra of raw hemp fibers extracts, and **p** UV-vis spectra of raw hemp fibers extracts (3 h and 5 h)



attributed to the bacterial growth inhibition of the MWE-DES treated fibers.

The main characteristic absorption of the chemical functional groups of flavonoids in the hemp extracts was recorded at 4000–799 cm^{-1} in the FTIR spectra (Fig. 7o). The strong absorption peak of cannabis

flavonoids was observed at 3328 cm^{-1} and it was also the characteristic absorption peak of OH groups (3000–3700 cm^{-1}). The presence of the C–H stretching at the peak of 2926–2885 cm^{-1} confirmed the presence of the C–H structure in the hemp extract. The peaks at 1716–1640 cm^{-1} were attributed to the

Table 4 Bacterial colony-forming units (CFU) reduction% of untreated and treated fibers after 24 h incubation

System ID	Sample type	Number of colonies	Reduction (%)
A	Raw	15	—
B	Kraft	14	6
C	ChCl-U	0	0
D	ChCl-G	27	—80
E	ChCl-CA	26	—73
F	SA-U	24	—60
G	Sul-M	41	—173

carbonyl groups (C=O), suggesting the alcohol ring structure of flavonoid moieties in the hemp extract. The UV absorption peak (Fig. 7p) of hemp extract was observed at the wavelength of 218 nm for both 3 h and 5 h extract. Bioactive compounds such as chalcone, aurones, flavone, and flavanone moieties have an absorption peak below 280 nm in the UV spectrum (Hao et al. 2014). Therefore, the phenolic flavonoid structure was assigned to the wavelength at 218 nm in the UV spectrum. There was no significant difference was observed in the FT-IR and UV spectra for the 3 h and 5 h ethanol extract of hemp fibers, suggesting the presence of low content of bioactive compounds. However, the similar rate of bacterial growth inhibition of raw and MWE-DES treated fibers (against *E. coli*) also confirmed the presence of such bioactive compounds.

Conclusion

Bast hemp fibers were successfully degummed using a combined MWE-DES treatment. The synergistic effect of combined MWE-DES treatment was found to be capable of removing non-cellulosic components such as lignin, hemicellulose, amorphous cellulose, and impurities from the hemp bast fiber structure without damaging the cellulose structure. MWE-DES treated fibers had higher thermal stability (T_{max} of MWE-DES treated fibers shifted toward a higher temperature of 356 °C), lower residual lignin content (2.88% to 4.88%), and higher crystallinity (up to 83.27% for choline chloride and urea DES). The processing time for the MWE-DES treatment was only 5 min with less chemical consumption while kraft treatment required a high

amount of chemicals and a longer process time (3 h). The higher yield of cellulose and high crystallinity of choline chloride-urea DES-treated fibers among other DESs can be attributed to the lower viscosity, high amount of competing hydrogen bond formation in the DES network, and uniform dispersion of microwave heating that facilitate the breakage of LCC linkages. However, the generation of wastewater in alkali degumming treatment possess a serious threat to the environment. On the other hand, a combined MWE-DES treatment offered an eco-friendly and one-pot, and single-step degumming treatment method. DES components are abundant, renewable, and inexpensive, and thus MWE-DES treatment offered an economical treatment of hemp fibers as compared to that of alkali treatment. Besides, the enhanced thermal stability, higher cellulose content, and higher crystallinity of MWE-DES-treated fibers were also comparable with those from the alkali-treated hemp fibers. Henceforth, the MWE-DES treated fibers can be used in textiles without any further bleaching treatment.

Author contributions All authors contributed to the study conception and design. Material preparation, data collection and analysis were performed by Bulbul Ahmed. The first draft of the manuscript was written by Bulbul Ahmed and all authors reviewed and commented on previous versions of the manuscript. All authors read and approved the final manuscript.

Funding The authors acknowledge the financial support by Louisiana Board of Regents [LEQSF (2020–23)-RD-B-02], National Science Foundation [2120640], National Institute of Forest Science, Seoul, Korea (FP0701-2021-02), and LSU LIFT Program.

Data availability The datasets used and/or analyzed during the current study are available from the corresponding author on reasonable request.

Declarations

Conflict of interest The authors declare no competing financial interest.

Ethics approval and consent to participate Not applicable.

Consent for publication Not applicable.

References

Abbott AP, Boothby D, Capper G, Davies DL, Rasheed RK (2004) Deep eutectic solvents formed between choline

chloride and carboxylic acids: versatile alternatives to ionic liquids. *J Am Chem Soc* 126(29):9142–9147. <https://doi.org/10.1021/ja048266j>

Ahmed B (2021) Degumming of Hemp Fibers Using Combined Microwave Energy and Deep Eutectic Solvent. Louisiana State University, Baton Rouge

Ahmed B, Wu Q, Lin H, Gwon J, Negulescu I, Cameron B (2022) Degumming of hemp fibers using combined microwave energy and deep eutectic solvent treatment. *Ind Crops Prod* 184:115046. <https://doi.org/10.1016/j.indcrop.2022.115046>

Baruah J, Nath BK, Sharma R, Kumar S, Deka RC, Baruah DC, Kalita E (2018) Recent trends in the pretreatment of lignocellulosic biomass for value-added products. *Front Energy Res* 6:141. <https://doi.org/10.3389/fenrg.2018.00141>

Bateni H, Saraeian A, Able C (2017) A comprehensive review on biodiesel purification and upgrading. *Biofuel Res J* 4(3):668–690. <https://doi.org/10.18331/BRJ2017.4.3.5>

Behera S, Gautam RK, Mohan S, Chattopadhyay A (2021) Hemp fiber surface modification: Its effect on mechanical and tribological properties of hemp fiber reinforced epoxy composites. *Polym Compos* 42(10):5223–5236. <https://doi.org/10.1002/pc.26217>

Chen Z, Wan C (2018) Ultrafast fractionation of lignocellulosic biomass by microwave-assisted deep eutectic solvent pretreatment. *Bioresour Technol* 250:532–537. <https://doi.org/10.1016/j.biortech.2017.11.066>

Cui Q, Li J, Yu C (2021) Optimization and characterization of flavonoids extracted from *Cannabis sativa* fibers. *Text Res J* 92(15–16):2886–2894. <https://doi.org/10.1177/0040175211027796>

French AD (2014) Idealized powder diffraction patterns for cellulose polymorphs. *Cellulose* 21(2):885–896. <https://doi.org/10.1007/s10570-013-0030-4>

Ghosh S, Cherkawi N, Hamad B (2020) Studies on hemp and recycled aggregate concrete. *Int J Concr Struct Mater* 14(1):1–17. <https://doi.org/10.1186/s40069-020-00429-6>

Hao XM, Yang Y, An LX, Wang JM, Han L (2014) Study on antibacterial mechanism of hemp fiber. *Adv Mat Res* 887–888:610–613. <https://doi.org/10.4028/www.scientific.net/AMR.887-888.610>

Hartati I, Sulistyo H, Sediawan WB, Azis MM, Fahrurrozi M (2021) Microwave-assisted urea-based-hydrotropic pretreatment of rice straw: experimental data and mechanistic kinetic models. *ACS Omega* 6(20):13225–13239. <https://doi.org/10.1021/acsomega.1c01084>

Huang X (2018) Bio-based Polyurethane Foams Made from Microwave Liquefaction of Biomass. Louisiana State University, Baton Rouge

Iseppi R, Brightenti V, Licata M, Lambertini A, Sabia C, Messi P, Pellati F, Benvenuti S (2019) Chemical characterization and evaluation of the antibacterial activity of essential oils from fibre-type *Cannabis sativa* L. (Hemp). *Molecules* 24(12):2302

Jung S-J, Kim S-H, Chung I (2015) Comparison of lignin, cellulose, and hemicellulose contents for biofuels utilization among 4 types of lignocellulosic crops. *Biomass Bioenergy* 83:322–327. <https://doi.org/10.1016/j.biombioe.2015.10.007>

Kabir MM, Wang H, Lau KT, Cardona F (2013) Effects of chemical treatments on hemp fibre structure. *Appl Surf Sci* 276:13–23. <https://doi.org/10.1016/j.apsusc.2013.02.086>

Kostic M, Pejic B, Skundric P (2008) Quality of chemically modified hemp fibers. *Bioresour Technol* 99(1):94–99. <https://doi.org/10.1016/j.biortech.2006.11.050>

Kostic MM, Pejic BM, Asanovic KA, Aleksić VM, Skundric PD (2010) Effect of hemicelluloses and lignin on the sorption and electric properties of hemp fibers. *Ind Crops Prod* 32(2):169–174. <https://doi.org/10.1016/j.indcrop.2010.04.014>

Kostryukov SG, Petrov PS, Kalyazin VA, Masterova YY, Tezikova VS, Khuchina NA, Labzina LY, Alalvan DK (2021) Determination of lignin content in plant materials using solid-state ¹³C NMR spectroscopy. *Polym Sci Ser B* 63(5):544–552. <https://doi.org/10.1134/S156009042050067>

Kumar N, Muley PD, Boldor D, Coty GG, Lynam JG (2019) Pretreatment of waste biomass in deep eutectic solvents: conductive heating versus microwave heating. *Ind Crops Prod* 142:111865. <https://doi.org/10.1016/j.indcrop.2019.111865>

Lee CBTL, Wu TY, Ting CH, Tan JK, Siow LF, Cheng CK, Jahim JM, Mohammad AW (2019) One-pot furfural production using choline chloride-dicarboxylic acid based deep eutectic solvents under mild conditions. *Bioresour Technol* 278:486–489. <https://doi.org/10.1016/j.biortech.2018.12.034>

Li Y, Tseng N, Li T, Liu H, Yang R, Gai X, Wang H, Shan S (2019) Microwave assisted hydrothermal preparation of rice straw hydrochars for adsorption of organics and heavy metals. *Bioresour Technol* 273:136–143. <https://doi.org/10.1016/j.biortech.2018.10.056>

Liu M, Fernando D, Meyer AS, Madsen B, Daniel G, Thygesen A (2015) Characterization and biological deactivation of hemp fibers originating from different stem sections. *Ind Crops Prod* 76:880–891. <https://doi.org/10.1016/j.indcrop.2015.07.046>

Liu Y, Chen DW, Xia Q, Guo B, Wang PQ, Liu PS, Liu PY, Li PJ, Yu PH (2017) Efficient cleavage of lignin–carbohydrate complexes and ultrafast extraction of lignin oligomers from wood biomass by microwave-assisted treatment with deep eutectic solvent. *Chemsuschem* 10(8):1692–1700. <https://doi.org/10.1002/cssc.201601795>

Liu C, Li M-C, Mei C, Xu W, Wu Q (2020) Rapid preparation of cellulose nanofibers from energy cane bagasse and their application as stabilizer and rheological modifiers in magnetorheological fluid. *ACS Sustain Chem Eng* 8(29):10842–10851. <https://doi.org/10.1021/acssuschemeng.0c02904>

Lyu P, Zhang Y, Wang X, Hurren C (2021) Degumming methods for bast fibers—a mini review. *Ind Crops Prod* 174:114158. <https://doi.org/10.1016/j.indcrop.2021.114158>

Manaia JP, Manaia AT, Rodrigues L (2019) Industrial hemp fibers: an overview. *Fibers* 7(12):106. <https://doi.org/10.3390/fib7120106>

Martins MA, Sosa FH, Kilpeläinen I, Coutinho JA (2022) Physico-chemical characterization of aqueous solutions

of superbase ionic liquids with cellulose dissolution capability. *Fluid Phase Equilib* 556:113414. <https://doi.org/10.1016/j.fluid.2022.113414>

Mijas G, Manich A, Lis M-J, Riba-Moliner M, Algaba I, Cayuela D (2021) Analysis of lignin content in alkaline treated hemp fibers: thermogravimetric studies and determination of kinetics of different decomposition steps. *J Wood Chem Technol* 41(5):210–219. <https://doi.org/10.1080/02773813.2021.1970185>

Mishra L, Das R, Mustafa I, Basu G, Gogoi N (2021) A novel approach of low alkali degumming of ramie. *J Nat Fibers* 18(6):857–866. <https://doi.org/10.1080/15440478.2019.1658257>

Murali B, Yogesh P, Karthickeyan N, Chandramohan D (2022) Multi-potency of bast fibers (flax, hemp and jute) as composite materials and their mechanical properties: a review. *Mater Today Proc* 62:1839–1843. <https://doi.org/10.1016/j.matpr.2022.01.001>

Nie K, Liu B, Zhao T, Wang H, Song Y, Ben H, Ragauskas AJ, Han G, Jiang W (2020) A facile degumming method of kenaf fibers using deep eutectic solution. *J NR Fibers* 19:1115–1125. <https://doi.org/10.1080/15440478.2020.1795778>

Nogueira CDC, Padilha CEDA, Santos ESD (2021) Enzymatic hydrolysis and simultaneous saccharification and fermentation of green coconut fiber under high concentrations of ethylene oxide-based polymers. *Renew Energy* 163:1536–1547. <https://doi.org/10.1016/j.renene.2020.10.050>

Pejic BM, Kostic MM, Skundric PD, Praskalo JZ (2008) The effects of hemicelluloses and lignin removal on water uptake behavior of hemp fibers. *Bioresour Technol* 99(15):7152–7159. <https://doi.org/10.1016/j.biortech.2007.12.073>

Ralph J, Lapierre C, Boerjan W (2019) Lignin structure and its engineering. *Curr Opin Biotechnol* 56:240–249. <https://doi.org/10.1016/j.copbio.2019.02.019>

Raza M, Abu-Jdayil B (2022) Cellulose nanocrystals from lignocellulosic feedstock: a review of production technology and surface chemistry modification. *Cellulose* 29:685–722. <https://doi.org/10.1007/s10570-021-04371-y>

Segal L, Creely JJ, Martin A Jr, Conrad C (1959) An empirical method for estimating the degree of crystallinity of native cellulose using the X-ray diffractometer. *Text Res J* 29(10):786–794. <https://doi.org/10.1177/004051755902901003>

Smith EL, Abbott AP, Ryder KS (2014) Deep eutectic solvents (DESs) and their applications. *Chem Rev* 114(21):11060–11082

Sorn V, Chang K-L, Phitsawan P, Ratanakhanokchai K, Dong C-D (2019) Effect of microwave-assisted ionic liquid/acidic ionic liquid pretreatment on the morphology, structure, and enhanced delignification of rice straw. *Bioresour Technol* 293:121929. <https://doi.org/10.1016/j.biortech.2019.121929>

Soumya KV, Shackleton CM, Setty SR (2019) Impacts of gum-resin harvest and *Lantana camara* invasion on the population structure and dynamics of *Boswellia serrata* in the Western Ghats. *India. for Ecol Manag* 453:117618. <https://doi.org/10.1016/j.foreco.2019.117618>

Stefanovic R, Ludwig M, Webber GB, Atkin R, Page AJ (2017) Nanostructure, hydrogen bonding and rheology in choline chloride deep eutectic solvents as a function of the hydrogen bond donor. *Phys Chem Chem Phys* 19(4):3297–3306. <https://doi.org/10.1039/C6CP07932F>

Subash MC, Muthiah P (2021) Eco-friendly degumming of natural fibers for textile applications: a comprehensive review. *Clean Eng Technol* 5:100304. <https://doi.org/10.1016/j.clet.2021.100304>

Tan YT, Chua ASM, Ngoh GC (2020) Deep eutectic solvent for lignocellulosic biomass fractionation and the subsequent conversion to bio-based products—A review. *Biore sour Technol* 297:122522. <https://doi.org/10.1016/j.biortech.2019.122522>

Tanăsă F, Zănoagă M, Teacă CA, Nechifor M, Shahzad A (2020) Modified hemp fibers intended for fiber-reinforced polymer composites used in structural applications—a review I methods of modification. *Polym Compos* 41(1):5–31. <https://doi.org/10.1002/pc.25354>

Thi S, Lee KM (2019) Comparison of deep eutectic solvents (DES) on pretreatment of oil palm empty fruit bunch (OPEFB): Cellulose digestibility, structural and morphology changes. *Bioresour Technol* 282:525–529. <https://doi.org/10.1016/j.biortech.2019.03.065>

Vărban R, Crișan I, Vărban D, Ona A, Olar L, Stoie A, Ștefan R (2021) Comparative FT-IR prospecting for cellulose in stems of some fiber plants: flax, velvet leaf. *Hemp Jute Appl Sci* 11(18):8570. <https://doi.org/10.3390/app11188570>

Viscusi G, Barra G, Gorrasí G (2020) Modification of hemp fibers through alkaline attack assisted by mechanical milling: effect of processing time on the morphology of the system. *Cellulose* 27(15):8653–8665. <https://doi.org/10.1007/s10570-020-03406-0>

Wang J, Zhao Y, Cai X, Tian M, Qu L, Zhu S (2020) Micro-wave-assisted One-step Degumming and Modification of Hemp Fiber with Graphene Oxide. *J Nat Fibers* 19(2):416–423. <https://doi.org/10.1080/15440478.2020.1745121>

Xu H, Peng J, Kong Y, Liu Y, Su Z, Li B, Song X, Liu S, Tian W (2020) Key process parameters for deep eutectic solvents pretreatment of lignocellulosic biomass materials: a review. *Bioresour Technol* 310:123416. <https://doi.org/10.1016/j.biortech.2020.123416>

Yu W, Wang C, Yi Y, Zhou W, Wang H, Yang Y, Tan Z (2019) Choline chloride-based deep eutectic solvent systems as a pretreatment for nanofibrillation of ramie fibers. *Cellulose* 26(5):3069–3082. <https://doi.org/10.1007/s10570-019-02290-7>

Publisher's Note Springer Nature remains neutral with regard to jurisdictional claims in published maps and institutional affiliations.

Springer Nature or its licensor (e.g. a society or other partner) holds exclusive rights to this article under a publishing agreement with the author(s) or other rightsholder(s); author self-archiving of the accepted manuscript version of this article is solely governed by the terms of such publishing agreement and applicable law.